Geophys. J. R. astr. Soc. (1982) **69**, 369–382

Implications of stress concentration on a strike-slip fault in an elastic plate subject to basal shear stress

M. Bonafede* and **M. Dragoni** *Istituto di Geofisica, Università di Bologna, 46, Via Irnerio-40126 Bologna, Italy*

Received 1981 September 21; in original form 1981 May 11

Summary. We consider a long strike-slip fault in a lithosphere modelled as an elastic slab. To the base of the slab a shear stress distribution is applied which simulates the viscous drag exerted by the asthenosphere. The resulant stress on the fault plane may directly fracture the lithosphere in its brittle upper portion; alternatively it may give rise at first to a stable aseismic sliding in the lower portion. In the latter case, stress concentration due to the deep aseismic slip is the relevant feature of the pre-seismic stress acting on the upper section of the lithosphere. The two cases are examined by use of dislocation theory and their observable effects compared. Different depths of the aseismic slip zone and the presence or absence of a uniform friction on the seismic fault are allowed for. If the model is applied to the San Andreas fault region, where a steady sliding condition actually seems to be present at shallow depth, it turns out that the slip amplitudes commonly associated with large earthquakes are consistent with average basal stress values which can be substantially lower than a few bars, a value often quoted as the steady state basal stress due to a velocity gradient in the upper asthenosphere.

1 Introduction

In the study of the coupling between the lithosphere and the asthenosphere and its effects on the seismic mechanism, two-dimensional models, in which an elastic slab lies over a viscoelastic half-space, have often been proposed (see, e.g. Rundle & Jackson 1977).

The value of the basal shear stress applied by the asthenosphere to the base of the lithosphere is a critical parameter in determining the relative importance of driving forces responsible for plate motion (Forsyth & Uyeda 1975). Let τ_b and τ_e be the average stresses acting on the plate base and edges respectively. If the viscous drag of the asthenosphere is responsible for this stress, we should have at equilibrium a relation between τ_b and τ_e which we can roughly write as

$$\tau_b Y^2 = ZY\tau_e \tag{1}$$

for a square plate with thickness Z and half-length Y. Lower bounds for edge stresses can be

*Also at Dipartimento di Scienze della Terra, Università di Ancona, Italy.

inferred from stress drops of interplate earthquakes (10–100 bar); resisting stresses may be much larger (Hanks 1977) and τ_e may reach values of several hundred bars.

Independent estimates of τ_b can be obtained from studies of the asthenosphere rheology (Melosh 1977). Most estimates of the viscosity of the upper asthenosphere are based on the assumption of Newtonian rheology and yield values which vary by two or three orders of magnitude. In fact, the values of τ_b obtained vary from 0.3 to 600 bar depending on the values assumed for the viscosity and thickness of the asthenosphere. Estimates based on the assumption of a non-Newtonian rheology (Melosh 1976a, b) impose much more restricted bounds, $\tau_b \simeq 2$–3 bar. Such low values seem to imply that basal stresses might be negligible in determining plate motion, particularly for smaller plates. The previous argument assumes that a perimetral stress as high as inferred from earthquake stress drops acts almost uniformly on the whole plate margin (however, we know that aseismic creep continuously relieves the edge stress on some fault sections, as is well documented for the San Andreas fault – see, e.g. Turcotte 1977).

Furthermore, geodetic measurements in the San Andreas fault region (Savage & Burford 1973, see also Thatcher 1975a, b) and the apparent absence of earthquake foci below about 15 km (Barker 1976) suggest that in the lower lithosphere 'the plates slip past one another fairly uniformly along a steep contact; ... along some fault segments fault creep occurs at the surface; this behaviour probably represents an extension of the area of stable sliding on the fault surface upward through the entire crust ... In other regions the upper portion of the fault surface appears to be locked ...' (from Savage & Burford 1973). It appears then that the right side of equation (1) is severely inadequate to represent the contribution of edge stresses to the equilibrium condition, since the lithospheric thickness Z ought to be replaced by a much smaller value representative of the width of the locked sections of plate margins.

The rheological and geochemical implications of this stable sliding condition have been investigated by Yuen *et al.* (1978), who show that a narrow zone of intense shear deformation due to viscous slip can be present along major transform faults and subducting slabs.

Below the locked section, a stress concentration pattern is originated by the steady sliding condition (Turcotte & Spence 1974, see also Savage 1975 and Turcotte & Spence 1975), whose influence on seismic rupture has been considered in a previous paper (Bonafede & Dragoni 1981).

In the present paper we try to derive conclusions on the basal shear stress from seismic slip and ground deformation measured at the Earth's surface. To this aim we assume that a basal shear stress drives the aseimsic steady slip envisaged in the Savage & Burford (1973) model. This region of continuous stable sliding is modelled as a vertical crack embodied in the lower lithosphere. The stress concentration thus created around the upper crack edge adds to the basal stress in determining the initial conditions for a seismic dislocation to take place on locked fault sections in the upper, brittle lithosphere. The relation between basal traction, seismic stress drop and resisting stress at transform boundaries has been already discussed by Hanks (1977) employing a simplified model of the lithosphere and of the stable sliding region.

2 The model

We consider the lithosphere as an elastic slab. At the base of this slab a stress distribution is applied which represents the effect of viscous motions within the asthenosphere. The model is illustrated in Fig. 1. A long strike-slip fault lies on the plane $x_2=0$, from the Earth's surface ($x_3=0$) to a depth a. The slab thickness is Z. While most models simply assume a

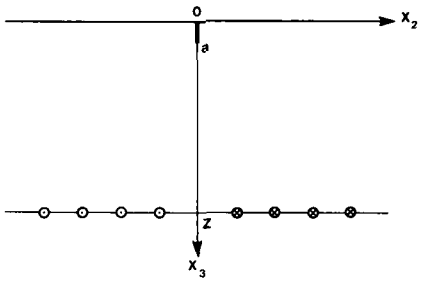

Figure 1. A section of the lithosphere at the fault region as modelled in the present paper. Conventional arrowheads and tails on the plane $x_3 = Z$ indicate the asthenospheric drag force depicted in Fig. 2.

uniform shear stress applied on the fault from remote boundaries at infinity, we assign a specific flow pattern at the top of the asthenosphere, which is responsible for the drag force on the lithosphere. In particular we suppose that the fault is situated above the boundary between two adjacent convective cells in which a steady plastic flow occurs horizontally in opposite directions.

2.1 THE ASTHENOSPHERIC DRAG

We assume that the asthenosphere ($x_3 > Z$) applies on the lithospheric base ($x_3 = Z$) a steady shear stress

$$\tau_{31}(x_2, Z-) = 6\tau_b\left[\frac{x_2}{Y} - \left(\frac{x_2}{Y}\right)^2 \operatorname{sgn} x_2\right], \qquad |x_2| \leqslant Y \tag{2}$$

which has a parabolic shape on both sides of the x_1-axis; Y is the characteristic horizontal half-length of either plate (Fig. 2). It can be seen from equation (2) that the average basal stress is τ_b in the interval $0 \leqslant x_2 \leqslant Y$ and $-\tau_b$ in the interval $-Y \leqslant x_2 \leqslant 0$. This may be obviously connected with a velocity field $\vec{v}$ in an asthenosphere behaving as a Newtonian viscous 'fluid': in this case

$$\tau_{31}(x_2, Z-) = \eta \left.\frac{\partial v_1}{\partial x_3}\right|_{x_3 = Z} \tag{3}$$

where η is the viscosity of the asthenosphere.

The model being two-dimensional, we assume antiplane strain

$$u_2 = u_3 = 0, \qquad \frac{\partial u_1}{\partial x_1} = 0 \tag{4}$$

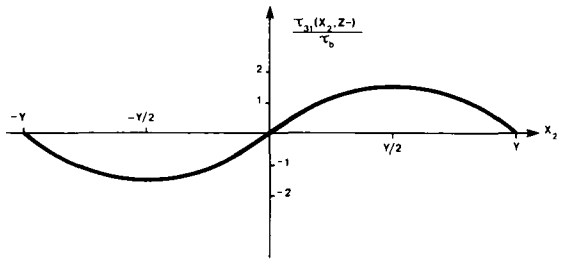

Figure 2. The basal shear stress $\tau_{31}(x_2, Z-)$ on the base of the lithosphere. Stress is uniform in the x_1-direction.

where $\vec{u}$ is the displacement field in the lithosphere. We take free-surface boundary conditions both on the plane $x_3=0$ (the Earth's surface) and on the plane $x_3=Z$ outside the range $|x_2| < Y$:

$$\tau_{31}(x_2, 0) = 0 \tag{5a}$$

$$\tau_{31}(x_2, Z) = 0, \quad |x_2| > Y. \tag{5b}$$

The stress pattern in $|x_2| < Y$ is specified in equation (2). As it will become clear in the following, condition (5b) is pertinent to the drag force distribution (equation 6) which yields the stress given in equation (2). Displacements and stresses produced in the lithosphere by the asthenospheric drag given in equation (2) are in fact equivalent to those due to a distribution of single-force strain nuclei (see, e.g. Love 1944)

$$\vec{F}(x_2, x_3) = 2\tau_{31}(x_2, Z-)\,\delta(x_3 - Z)\,\hat{x}_1, \quad |x_2| < Y. \tag{6}$$

Computation of the displacement produced by this distribution in an unbounded elastic space is performed by integrating the right side of equation (6) with the displacement field due to an infinite linear uniform distribution of single forces with unit intensity and direction x_1. Such a distribution placed along a line $x_2=y, x_3=Z$ gives rise to a displacement

$$u_1(x_2, x_3) = -\frac{1}{4\pi\mu}\log\left[(x_2 - y)^2 + (x_3 - Z)^2\right] \tag{7}$$

where μ is the rigidity of the elastic medium. Non-vanishing stress components τ_{21} and τ_{31} are calculated consequently from Hooke's law:

$$\tau_{i1} = \mu\frac{\partial u_1}{\partial x_i} \qquad (i = 2, 3).$$

A similar approach was used in Bonafede & Dragoni (1981). Displacements and stresses in the slab, $0 < x_3 < Z$, are obtained by simply superimposing an infinite number of image force distributions placed on the planes $x_3=(2n+1)Z$, $n=\pm1, \pm2, \ldots, \pm\infty$. The total stress field satisfies the boundary conditions (2) and (5). What is of main interest to us is the stress component τ_{21} acting on the fault plane $x_2=0$. By straightforward calculation

$$\tau_{21}(0, x_3) = \frac{6\tau_b}{\pi}\sum_{n=-\infty}^{\infty}\left\{1 - 2\frac{x_3 - Z_n}{Y}\arctan\frac{Y}{x_3 - Z_n} + \left(\frac{x_3 - Z_n}{Y}\right)^2\log\left[1 + \left(\frac{Y}{x_3 - Z_n}\right)^2\right]\right\} \tag{8}$$

where $Z_n = (2n+1)Z$. We now introduce the notation

$$\tau_0 = \tau_{21}(0, 0)$$

$$\tau_Z = \tau_{21}(0, Z). \tag{9}$$

Assuming for Z and Y values appropriate to a large plate:

$$Z = 100\,\text{km},$$

$$Y = 4000\,\text{km} \tag{10}$$

we get $(\tau_Z - \tau_0)/\tau_Z \simeq 0.2$ per cent, i.e. the stress varies very little on the fault plane. Thus we are allowed to take a uniform shear stress between $x_3=0$ and $x_3=a$ and we put it equal to

τ_0 for a seismic dislocation to take place in the upper lithosphere. The deformation produced at the Earth's surface by the asthenospheric drag (equation 2) is also fairly uniform along the x_2-axis as long as the distance from the fault is much less than the plate half-length Y.

2.2 A SEISMIC DISLOCATION IN A UNIFORM STRESS FIELD

First, we look at what happens if a dislocation originates on the fault due to direct asthenosphere-induced stress only. We assume crack-like boundary conditions on the fault faces, i.e. the dislocation completely relieves the applied stress; friction is neglected. The influence of a residual stress on the fault will be considered in a later section.

A way to obtain displacement and stress fields of a crack subjected to anti-plane shear stress τ_{21} in an *unbounded elastic medium* is to solve the integral equation

$$\tau_{21}(0,x_3) - \frac{\mu b}{2\pi} \int_{-a}^{a} \frac{\mathscr{D}(\zeta)}{x_3 - \zeta}\, d\zeta = 0, \qquad |x_3| < a \tag{11}$$

which gives the distribution $\mathscr{D}(x_3)$ of infinitesimal screw dislocations equivalent to the crack. Here b is the Burgers vector of an infinitesimal dislocation and the slash on the integral sign denotes Cauchy principal value. The solution to equation (11) is given by (see, e.g. Bilby & Eshelby 1968)

$$\mathscr{D}(x_3) = -\frac{2}{\pi\mu b} \frac{1}{\sqrt{a^2 - x_3^2}} \int_{-a}^{a} \frac{\sqrt{a^2 - \zeta^2}}{x_3 - \zeta}\, \tau_{21}(0,\zeta)\, d\zeta, \qquad |x_3| < a. \tag{12}$$

From $\mathscr{D}(x_3)$ we can calculate the displacement discontinuity

$$\Delta u(x_3) = b \int_{-a}^{x_3} \mathscr{D}(\zeta)\, d\zeta, \qquad |x_3| \leqslant a, \tag{13}$$

the seismic moment and the energy release

$$M = \mu L \int_{-a}^{a} \Delta u(x_3)\, dx_3, \tag{14}$$

$$\Delta E = -\frac{L}{2} \int_{-a}^{a} \Delta u(x_3)\, \tau_{21}(0,x_3)\, dx_3, \tag{15}$$

where L is the fault length ($L \gg a$ by assumption). The released stress and strain field components are given by

$$\sigma_{i1}(x_2,x_3) = \int_{-a}^{a} \mathscr{D}(\zeta)\, \sigma_{i1}^{s}(x_2, x_3 - \zeta)\, d\zeta \tag{16}$$

$$e_{i1}(x_2,x_3) = \frac{1}{2\mu}\, \sigma_{i1}(x_2,x_3) \tag{17}$$

where $i = 2, 3$ and the σ_{i1}^{s} are the non-vanishing stress components due to an infinitesimal screw dislocation placed in $x_2 = 0, x_3 = \zeta$.

The results for a uniform applied stress are simple to obtain and have been reported by several authors (e.g. Bilby & Eshelby 1968). These results are immediately applicable to a *half-space* ($x_3 > 0$ in our case), because the stress component σ_{31} of the crack vanishes on the

plane $x_3=0$, owing to the symmetry of the problem. Since we know that the asthenosphere behaves elastically for short times, we take just such half-space solution, neglecting the difference between the lithospheric and the asthenospheric rigidities.

The expressions for the relevant quantities of the single dislocation problem (I) are the following:

$$\Delta u^{\mathrm{I}}(x_3) = 2\tau_0\sqrt{a^2 - x_3^2}/\mu, \quad 0 \leq x_3 \leq a \tag{18}$$

$$M^{\mathrm{I}} = \pi a^2 \tau_0/2, \tag{19}$$

$$\Delta E^{\mathrm{I}} = -\tau_0 M^{\mathrm{I}}/(2\mu), \tag{20}$$

$$\begin{cases} \sigma_{21}^{\mathrm{I}} = \tau_0\left[\dfrac{r}{\sqrt{r_1 r_2}}\cos(\theta-\phi) - 1\right], & (21) \\ \sigma_{31}^{\mathrm{I}} = \tau_0 \dfrac{r}{\sqrt{r_1 r_2}}\sin(\theta-\phi), & (22) \end{cases}$$

where $\phi=(\theta_1+\theta_2)/2$ and $|\theta| \leq \pi/2$. The coordinates used for the stress field are defined in Fig. 3.

The strain at the Earth's surface is

$$e_{21}^{\mathrm{I}}(x_2, 0) = \frac{\tau_0}{2\mu}\left(\frac{|x_2|}{\sqrt{x_2^2 + a^2}} - 1\right). \tag{23}$$

The stress component σ_{31} obviously modifies the pre-seismic stress pattern at the lithosphere base (equation 2) and we may suppose that the original value for the drag force will be restored by the asthenospheric flow only after a characteristic time η/μ.

2.3 INTRODUCTION OF AN ASEISMIC DISLOCATION

Introduction of the values (10) for Z and Y in the relations (18)–(23), with $\tau_b = 2$ bar as inferred by Melosh (1976a, b), yields values commonly accepted for a large earthquake along the San Andreas fault. If, however, we take into account that a condition of stable aseismic sliding prevails under the locked section of the fault, as discussed in the introduction, we are led to think that the first effect of the asthenospheric drag is the creation of an aseismic

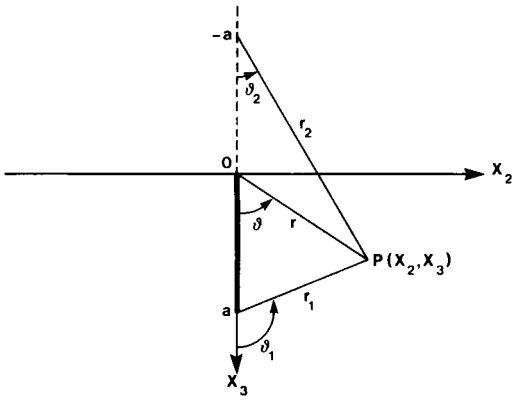

Figure 3. The coordinate system employed for the seismic dislocation stress field.

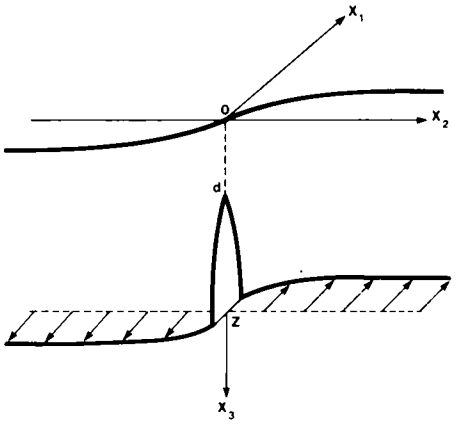

Figure 4. The aseismic dislocation. The arrows on the plane $x_3 = Z$ denote the displacement field.

dislocation in the lower part of the lithosphere, $d \leqslant x_3 \leqslant Z$, $d > a$, on the same fault plane $x_2 = 0$ (Fig. 4). This aseismic dislocation is a schematic representation of the narrow zone of intense shear deformation envisaged by Yuen *et al.* (1978).

We approximate the shear stress produced by the asthenosphere on the lower aseismic section of the fault with a uniform stress τ_Z as given by equation (9). Displacement and stress due to the aseismic dislocation in the lithospheric slab are obtainable by modifying for anti-plane strain a solution given by Koiter (1959). They are given in terms of a complex variable $z = x_3 + ix_2$:

$$u_1^{\mathrm{A}}(x_2, x_3) = \frac{\tau_Z}{\mu}\left(\frac{2Z}{\pi}\log\frac{\left|\sin(\pi z/2Z) + \sqrt{\sin^2(\pi z/2Z) - \sin^2(\pi d/2Z)}\right|}{\sin(\pi d/2Z)} - x_2\right) \tag{24}$$

$$\sigma_{21}^{\mathrm{A}}(x_2, x_3) = -\tau_Z\left\{1 + \mathrm{Im}\left[\cos\frac{\pi z}{2Z}\left(\sin^2\frac{\pi z}{2Z} - \sin^2\frac{\pi d}{2Z}\right)^{-1/2}\right]\right\} \tag{25}$$

$$\sigma_{31}^{\mathrm{A}}(x_2, x_3) = \tau_Z\,\mathrm{Re}\left[\cos\frac{\pi z}{2Z}\left(\sin^2\frac{\pi z}{2Z} - \sin^2\frac{\pi d}{2Z}\right)^{-1/2}\right]. \tag{26}$$

This solution satisfies the boundary conditions, equations (2) and (5). The problem of a dislocation in the lower lithosphere has been worked out by Turcotte & Spence (1974) with the boundary conditions of uniform shear stress applied at infinity and vanishing traction on the whole plane $x_3 = Z$, so that their solution differs from the present one in its behaviour at large distances from the fault.

The displacement discontinuity and the energy release are

$$\Delta u^{\mathrm{A}}(x_3) = \frac{4Z}{\pi\mu}\tau_Z \log\left[\mathrm{cosec}\frac{\pi d}{2Z}\left(\sin\frac{\pi x_3}{2Z} + \sqrt{\sin^2\frac{\pi x_3}{2Z} - \sin^2\frac{\pi d}{2Z}}\right)\right], \quad d \leqslant x_3 \leqslant Z \tag{27}$$

$$\Delta E^{\mathrm{A}} = -\frac{2LZ^2}{\pi\mu}\tau_Z^2 \log\mathrm{cosec}\frac{\pi d}{2Z} \tag{28}$$

and the strain at the Earth's surface is

$$e_{21}^{\mathrm{A}}(x_2, 0) = \frac{\tau_Z}{2\mu}\left[\cosh\frac{\pi x_2}{2Z}\left(\sinh^2\frac{\pi x_2}{2Z} + \sin^2\frac{\pi d}{2Z}\right)^{-1/2} - 1\right]. \tag{29}$$

The consequence of introducing an aseismic dislocation is obviously a stress concentration on the locked section of the fault, $0 < x_3 < a$, which is the more pronounced the less the aseismic slip is distant from the Earth's surface. This is evident in Fig. 5, where we have plotted the total shear stress τ_{21}^{tot} on the seismic fault

$$\tau_{21}^{tot}(0,x_3) = \tau_0 + \sigma_{21}^{A}(0,x_3) \tag{30}$$

where

$$\sigma_{21}^{A}(0,x_3) = \tau_Z \left[\cos\frac{\pi x_3}{2Z} \left(\sin^2\frac{\pi d}{2Z} - \sin^2\frac{\pi x_3}{2Z} \right)^{-1/2} - 1 \right] \tag{31}$$

and $0 < x_3 < d$.

2.4 A SEISMIC DISLOCATION WITH STRESS CONCENTRATION

We look now for seismic slip on the locked section of the fault in the presence of the stress concentration produced by the aseismic dislocation (model II). The solution is obtained by calculating numerically the Cauchy integral in equation (12) with applied shear stress given by equation (30). The displacement discontinuity, seismic moment and energy release are also calculated numerically according to equations (13), (14) and (15) respectively.

These results can be put in the form

$$\Delta u^{II}(x_3) = a\tau_b \, \mathscr{U}(x_3)/\mu, \qquad 0 < x_3 < a \tag{32}$$

$$M^{II} = a^2 L \tau_b \, \mathscr{M} \tag{33}$$

$$\Delta E^{II} = -a^2 L \tau_b^2 \, \mathscr{E}/\mu \tag{34}$$

where $\mathscr{U}(x_3)$, $\mathscr{M}$ and $\mathscr{E}$ are non-dimensional quantities. $\mathscr{M}$ and $\mathscr{E}$ are given in Table 1.

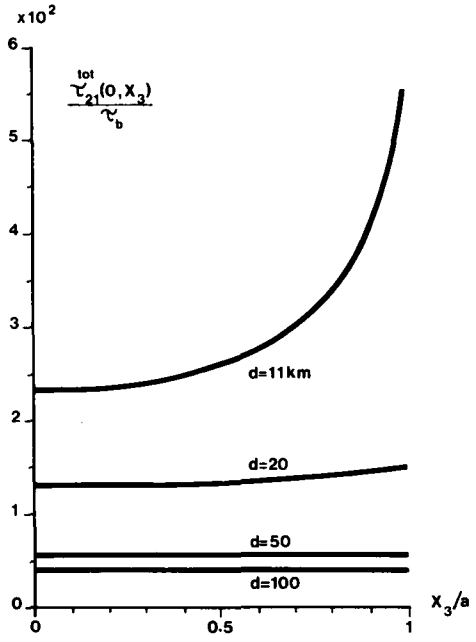

Figure 5. The total pre-seismic stress on the seismic section of the fault. The non-dimensional quantity $\tau_{21}^{tot}(0,x_3)/\tau_b$ is plotted.

Table 1. The non-dimensional seismic moment $\mathcal{M}$ and energy release $\mathcal{E}$ of the seismic dislocation for various values of d. Zero residual stress. $Y = 4000$ km, $Z = 100$ km, $a = 10$ km.

d (km)	$\mathcal{M}$ ($\times 10^2$)	$\mathcal{E}$ ($\times 10^{-2}$)
11	4.3	5.8
20	2.1	1.4
50	0.89	0.25
100	0.63	0.13

The strain e_{21}^{II} at the Earth's surface has been calculated numerically according to equations (17) and (16).

Model I (single dislocation) can be considered the limiting case of model II when $d \to Z$. Fig. 5 shows the initial stress field $\tau_{21}^{tot}(0, x_3)$ on the seismic fault surface. We see that the initial stress is practically uniform when $d = 100$ and $d = 50$ km, but a substantial non-uniformity of the initial stress appears on the seismic fault section if the aseismic dislocation tip reaches shallow depths.

The seismic dislocation amplitude $\mathcal{U}(x_3)$ is fairly sensitive to a change in the initial stress as is evident from Fig. 6, where the effect of a change in d on the vertical profiles $\mathcal{U}(x_3)$ is shown.

3 Discussion and conclusions

The previous arguments show how the presence of the aseismic dislocation affects the vertical trend of the stress field and the seismic dislocation amplitude. The values of such quantities, however, can be directly observed only in the proximity of the Earth's surface. Fig. 7 shows the ground deformation due to the aseismic dislocation along a horizontal traverse across the fault. The strain $e_{21}^{A}(x_2, 0)$ is normalized to the same maximum value in order to bring out the influence of the parameter d on deformation patterns. These strain profiles are the same that could be obtained from Turcotte & Spence's (1974) model, the difference arising when we compare total pre-seismic ground strains at large distances from

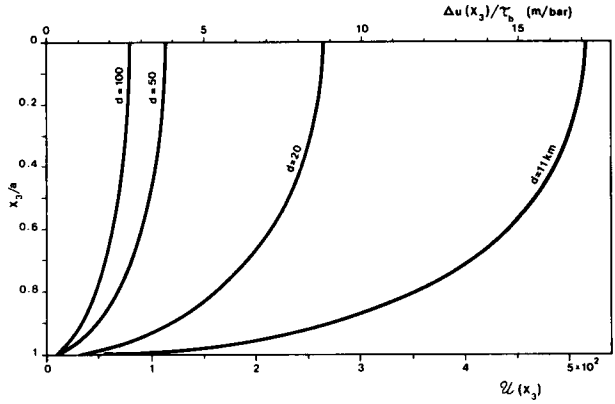

Figure 6. The non-dimensional slip amplitude $\mathcal{U}(x_3)$ (bottom scale) on the seismic section of the fault, for various values of d; $d = 100$ km stands for the absence of aseismic dislocation. The top scale shows values of $\Delta u(x_3)/\tau_b$ ($\mu = 3 \times 10^{11}$ dyne cm^{-2}, $a = 10$ km).

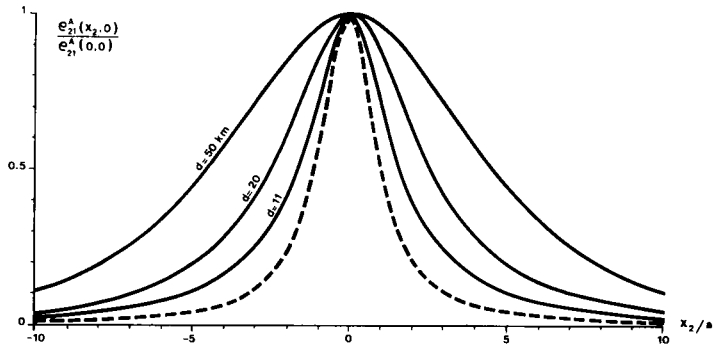

Figure 7. The ground deformations produced by the aseismic dislocation for different values of d. The dashed curve shows, for comparison, the ground deformation produced by the single screw dislocation model, for $d = 11$ km. Curves are normalized to the same maximum value.

the fault. The total ground strain is in fact obtained in our model by adding to $e_{21}^A(x_2, 0)$ the non-uniform ground strain $\tau_{21}(x_2, 0)/2\mu$ due to the asthenospheric drag. From Fig. 7 we note that, at least in principle, geodetic measurements can determine the depth d of the aseismic dislocation tip. Unfortunately the strain measurements across real faults do not allow any fine resolution, although the actual strain traverses vaguely resemble the trends displayed in Fig. 7 (Savage & Burford 1970, 1973; Thatcher 1975b).

A model of strain accumulation due to a buried strike-slip fault was already presented by Savage & Burford (1973). They employed a single screw dislocation placed at $x_3 = d$ in an elastic half-space, which corresponds to a step-function displacement discontinuity

$$\Delta u(x_3) = b\theta(x_3 - d) \tag{35}$$

(to be compared with our Somigliana dislocation – equation 27). Their model, while yielding a first estimate of the effect, is clearly an oversimplification. Unless the dislocation is very far from the Earth's surface, a single screw dislocation gives a ground strain which is considerably different from that of a Somigliana dislocation, whatever the choice for b may be. The normalized strain profile produced by the single screw dislocation model is shown in Fig. 7, for a value $d = 11$ km, for comparison with our model.

Fig. 8 shows how a change in d modifies the sudden ground deformation produced by the slip occurring on the seismic fault section: the greater slip amplitude associated with stress

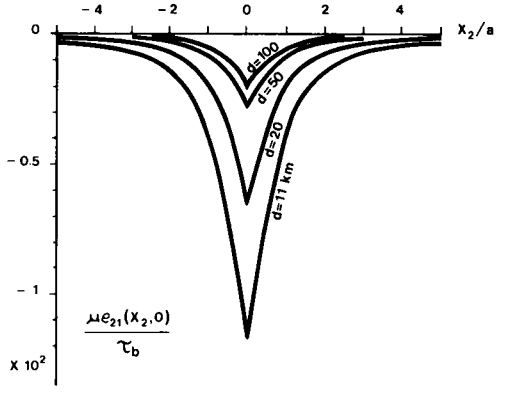

Figure 8. The ground deformation produced by the seismic dislocation for different values of d; $d = 100$ km means no aseismic dislocation. The non-dimensional quantity $\mu e_{21}(x_2, 0)/\tau_b$ is plotted.

concentration (see Fig. 6) obviously entails larger ground deformations in the proximity of the fault.

The question we wish to answer, on the basis of the previous considerations, is the following: once we accept that a stable sliding condition at low levels of stress is present at depth along major transform faults, what inference can be derived regarding the average value τ_b of the basal shear stress acting on the lithospheric plates? The discussion is restricted to the San Andreas fault, where several data are available for our purposes. We take $a = 10$ km, $Z = 100$ km, $Y = 4000$ km.

Looking at Fig. 6, we see that a surface slip in the order of 5 m (as observed in connection with the 1906 San Francisco earthquake) is attained for $\tau_b = 2$ bar in the absence of aseismic dislocation. If, however, stress concentration produced by the stable sliding regime below depth d is taken into account, we find lower estimates for τ_b: when $d = 11$ km, the average basal stress required for the observed displacement of the plate margin can be lower than 0.5 bar. In the limiting case of creep taking place at vanishing levels of stress, the viscous drag applied by the asthenosphere to the lithospheric base could be entirely responsible for the motion of larger plates.

The previous conclusions, however, are drawn in the absence of friction (or any residual stress) on the seismic dislocation surface. A simple friction model has been considered to overcome this limitation: we assume that a uniform residual stress τ_f is left on the seismic fault surface. It is to be mentioned, incidentally, that Weertman (1964) considered a dislocation model of the San Andreas fault with non-uniform friction. We write τ_f as a fraction α of the total pre-seismic stress τ_{21}^{tot} acting at the Earth's surface:

$$\tau_f = \alpha \tau_{21}^{tot}(0, 0). \tag{36}$$

Models I and II have been reconsidered with the boundary condition of a residual stress τ_f on the seismic dislocation surface. The distribution of infinitesimal dislocations relative to this case is still computed from equation (12), where the stress to be released on the seismic dislocation surface ($\tau_{21}(0, \zeta)$ in the absence of friction) is replaced by $\tau_{21}(0, \zeta) - \tau_f$. The other quantities are then calculated through the same steps as before.

The non-dimensional seismic slip $\mathscr{U}^f(x_3)$ and the ground deformation $e_{21}^f(x_2, 0)$ are shown in Figs 9 and 10 in the case $d = 11$ km, for various values of α. It is to be stressed that when α approaches 1 the maximum slip amplitude is attained at depth: this feature reflects

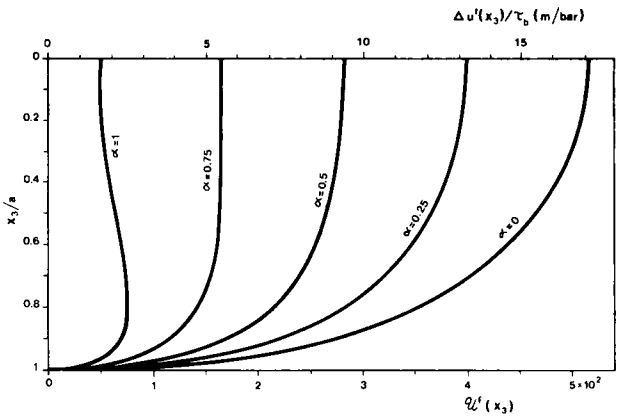

Figure 9. The non-dimensional slip amplitude $\mathscr{U}^f(x_3)$ (bottom scale) on the seismic section of the fault, for $d = 11$ km and different values of α. The top scale shows values of $\Delta u^f(x_3)/\tau_b$ ($\mu = 3 \times 10^{11}$ dyne cm^{-2}, $a = 10$ km).

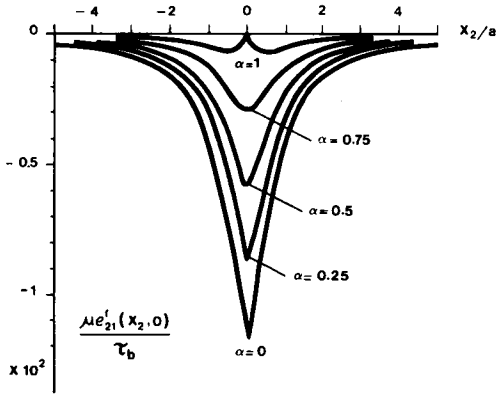

Figure 10. The ground deformation produced by the seismic dislocation in the presence of friction. The non-dimensional quantity $\mu e^f_{21}(x_2, 0)/\tau_b$ is plotted for $d = 11$ km and different values of α.

the vanishingly small stress available to drive the dislocation in the proximity of the Earth's surface, which also requires zero ground deformation on the fault trace. When $\alpha = 1$, slip still occurs on the seismic fault section, since at depth the driving stress of our model is still higher than frictional stress (see equations 30 and 36).

Table 2 shows the average basal stress τ_b needed for a surface slip of 5 m to take place in the presence of friction for various values of d. We can see that, in the presence of aseismic dislocation, τ_b values are always lower than 3 bar (the maximum value predicted by Melosh (1976a,b) on the basis of a non-Newtonian rheology for the asthenosphere) as long as the residual stress on the seismic dislocation surface does not exceed 100 bar. On the other hand, in the presence of a significant residual stress ($\tau_f > 100$ bar), small τ_b values are possible only when $d = 11$ km in Table 2. If, however, $d \gtrsim 20$ km, 5 m slip amplitudes could only be attained if τ_b is substantially greater than a few bars.

We have accordingly subdivided Table 2 into three regions: the region on the left gives residual stresses which are less than 100 bar; the other two regions contain respectively fault models with low τ_b values ($\tau_b \lesssim 3$ bar) up, and fault models with higher τ_b values down.

Since geodetic measurements and the apparent absence of earthquake foci below about 15 km on the San Andreas fault seem to deny that $d > 20$ km, if we admit that creep on deep fault sections can take place at very low levels of stress, we are almost inevitably led to conclude that an average basal shear stress lower than 3 bar is still capable of driving the motions of major tectonic plates (at least as we observed them at the Earth's surface in connection with greater earthquakes). If, however, the stable regime at depth prevails only when a significant stress threshold is exceeded, larger values can be accepted for the basal

Table 2. Values of the basal shear stress τ_b (in bar) as inferred from dislocation models with various values of d and α. $Y = 4000$ km, $Z = 100$ km, $a = 10$ km. The furthest right column shows, after multiplication by $\alpha\tau_b$, the corresponding values of residual stress on the *seismic* fault section (in bar). See the text for the subdivision in three regions.

d (km) \ α	0	0.25	0.50	0.75	1	$\tau_f/\alpha\tau_b$
11	0.3	0.4	0.5	0.9	3.1	233
20	0.6	0.8	1.1	2.1	27	129
50	1.3	1.8	2.7	5.3	1000	57
100	1.9	2.5	3.8	7.5		40

Table 3. Values of the basal shear stress τ_b (in bar) as inferred from dislocation models with various values of d and β. $Y = 4000$ km, $Z = 100$ km, $a = 10$ km. The furthest right column shows, after multiplication by $\beta\tau_b$, the corresponding values of residual stress on the *aseismic* fault section (in bar). No friction on the seismic fault section.

d (km) \ β	0	0.25	0.50	0.75	1	$\tau_r/\beta\tau_b$
11	0.3	0.4	0.5	0.8	–	40
20	0.6	0.7	0.9	1.2	–	40
50	1.3	1.4	1.6	1.7	–	40
100	1.9	1.9	1.9	1.9	1.9	40

shear stress. Let us assume that a residual stress τ_r is left on the aseismic dislocation surface: we write

$$\tau_r = \beta\tau_Z \tag{37}$$

where τ_Z is defined by equation (9) and $0 < \beta < 1$. In order that a surface slip of 5 m is attained, in the absence of friction on the seismic fault section ($\alpha = 0$), τ_b values as shown in Table 3 must be applied to the base of the lithosphere. We see that τ_b values (< 1.9 bar) requested in Table 2 for a certain value of d are consistent in Table 3 with a lower value of d, when $\beta > 0$. In conclusion, τ_b values derived according to our model depend on observable quantities (such as ground strain, slip and stress drop) through the two parameters α and β, which are poorly constrained. Accordingly, some degree of non-uniqueness in the previous inferences must be clearly recognized.

Some evident limitations of our dislocation models can moreover affect the previous conclusions. Among these, the assumption of a perfectly elastic lithosphere is probably inadequate to describe the region between the seismic and the aseismic dislocation ($a < x_3 < d$) where a high stress concentration is localized and, according to Yuen *et al.* (1978), an inelastic regime may prevail. This might modify the detailed stress concentration pattern at depth. A second limitation is implicitly present in classical dislocation models: the edges of a dislocation surface must be prescribed, while we reasonably expect that the seismic dislocation surface might, sooner or later, extend into the aseismic dislocation surface.

Bearing in mind both the previous limitations, conclusions for the post-seismic long-term deformation are not taken here (see, e.g. Savage 1975 and Turcotte & Spence 1974, 1975). A viscoelastic description of the asthenosphere is necessary to this end. Many authors have considered the effect of the asthenosphere rheology on strike-slip faults; however, some of them (e.g. Nur & Mavko 1974; Spence & Turcotte 1979) do not allow for the pre-seismic stable sliding condition at depth, while others (Savage & Prescott 1978) model it as a single screw dislocation and do not consider the details of the seismic events.

Acknowledgments

The authors wish to express their appreciation to Professors E. Boschi and G. Puppi for useful discussions and continuous encouragement throughout this work. They also wish to express their appreciation to Professor A. Zichichi for support.

References

Barker, T. G., 1976. Quasi-static motions near the San Andreas fault zone, *Geophys. J. R. astr. Soc.*, **45**, 689–706.

Bilby, B. A. & Eshelby, J. D., 1968. Dislocations and the theory of fracture, in *Fracture – an Advanced Treatise*, vol. 1, pp. 99–182, ed. Liebowitz, H., Academic Press, New York.

Bonafede, M. & Dragoni, M., 1981. On strike-slip dislocations in an elastic half-space in the presence of localized distributions of strain nuclei, *Geophys. J. R. astr. Soc.*, **67**, 77–90.

Forsyth, D. & Uyeda, S., 1975. On the relative importance of the driving forces of plate motion, *Geophys. J. R. astr. Soc.*, **43**, 163–200.

Hanks, T. C., 1977. Earthquake stress drops, ambient tectonic stresses and stresses that drive plate motions, *Pageoph.*, **115**, 441–458.

Koiter, W. T., 1959. An infinite row of collinear cracks in an infinite elastic sheet, *Ing.-Arch.*, **28**, 168–172.

Love, A. E. H., 1944. *A Treatise on the Mathematical Theory of Elasticity*, chapter 8, Dover, New York.

Melosh, H. J., 1976a. Non-linear stress propagation in the Earth's upper mantle, *J. geophys. Res.*, **81**, 5621–5632.

Melosh, H. J., 1976b. Plate motion and thermal instability in the asthenosphere, *Tectonophys.*, **35**, 363–390.

Melosh, H. J., 1977. Shear stress on the base of a lithospheric plate, *Pageoph.*, **115**, 429–439.

Nur, A. & Mavko, G., 1974. Postseismic viscoelastic rebound, *Science*, **183**, 204–206.

Rundle, J. B. & Jackson, D. D., 1977. A viscoelastic relaxation model for postseismic deformation, *Pageoph.*, **115**, 401–411.

Savage, J. C., 1975. Comment on "Analysis of strain accumulation on a strike-slip fault" by D. L. Turcotte and D. A. Spence, *J. geophys. Res.*, **80**, 4111–4114.

Savage, J. C. & Burford, R. O., 1970. Accumulation of tectonic strain in California, *Bull. seism. Soc. Am.*, **60**, 1877–1896.

Savage, J. C. & Burford, R. O., 1973. Geodetic determination of relative plate motion in central California, *J. geophys. Res.*, **78**, 832–845.

Savage, J. C. & Prescott, W. H., 1978. Asthenosphere readjustment and the earthquake cycle, *J. geophys. Res.*, **83**, 3369–3376.

Spence, D. A. & Turcotte, D. L., 1979. Viscoelastic relaxation of cyclic displacements on the San Andreas Fault, *Proc. R. Soc. A*, **365**, 121–144.

Thatcher, W., 1975a. Strain accumulation and release mechanism of the 1906 San Francisco earthquake, *J. geophys. Res.*, **80**, 4862–4872.

Thatcher, W., 1975b. Strain accumulation on the northern San Andreas fault zone since 1906, *J. geophys. Res.*, **80**, 4873–4880.

Turcotte, D. L., 1977. Stress accumulation and release on the San Andreas fault, *Pageoph.*, **115**, 413–427.

Turcotte, D. L. & Spence, D. A., 1974. An analysis of strain accumulation on a strike-slip fault, *J. geophys. Res.*, **79**, 4407–4412.

Turcotte, D. L. & Spence, D. A., 1975. Reply, *J. geophys. Res.*, **80**, 4115.

Weertman, J., 1964. Continuum distribution of dislocations on faults with finite friction, *Bull. seism. Soc. Am.*, **54**, 1035–1058.

Yuen, D. A., Fleitout, L., Schubert, G. & Froidevaux, C., 1978. Shear deformation zones along major transform faults and subducting slabs, *Geophys. J. R. astr. Soc.*, **54**, 93–119.